Supporting Information for

Efficient Way To Assemble CdS Nanorose-Decorated CdSe-Tetrakaidecahedron Heterojunction Photoanodes for High-Photoelectrochemical Performance

Mahadeo A. Mahadik[†], Hee-Suk Chung,[‡] Hyeon Ih Ryu,[‡] Weon-Sik Chae,[§] Min Cho[†], ** and Jum Suk Jang[†,]*

[†]Division of Biotechnology, Safety, Environment and Life Science Institute, College of Environmental and Bioresource Sciences, Chonbuk National University, Iksan 570-752, Republic of Korea.

[‡]Jeonju Center, Korea Basic Science Institute, Jeonju, Jeollabuk-do, 54907, Republic of Korea

[§]*Daegu Center, Korea Basic Science Institute, Daegu 41566, Republic of Korea*

*__Corresponding Authors__
E-mail: jangjs75@jbnu.ac.kr;
Tel.: +82 63 850 0846. Fax: +8263 850 0834.
**__Co-Corresponding Authors__
E-mail: cho317@jbnu.ac.kr (Min Cho).

Number of pages: 14
Number of Tables: 3
Number of figures: 11

Table of Contents	***Page#***
Table S1	S3-S4
Table S2	S4
Table S3	S4
Figure S1	S5
Figure S2	S5
Figure S3	S6
Figure S4	S8
Figure S5	S8
Figure S6	S9
Figure S7	S10
Figure S8	S11
Figure S9	S11
Figure S10	S12
Figure S11	S12
References	S13-S14

Table S1. Reports on the performances of CdSe based photocatalysts.

Photocatalysts	**method**	**Electrolyte**	**Performance**	**Application**	**Ref**
CdSe and CdSe/CdS core–shell QDs	rapid microwave activated approach	0.01 g/L Methyl orange	92% degradation of Methyl orange after 1h	Methyl orange Dye degradation	[1]
CdSe and CdSe(ZnS) Sol–Gel Thin Films (～70 nm Thick)	sol–gel and spin coating methods	0.1 M polysulfide aqueous solution (Na_2S + NaOH + S)	～250 μA cm^{-2} anodic photocurrent at −0.57 V	Photoelectrochemical measurements	[2]
CdSe−$_nC^{60}$ composite clusters deposited on optically transparent electrodes	Electrophoretic Deposition	0.1 M Na_2S	0.25 mA/cm^2 at 0.3 V	photocurrent response and stability	[3]
Phenothiazine - modified CdSe QDs electrode	ligand exchange approach	0.1 m Na_2SO_4	−180 μA cm^{-2} at −0.1 V vs. NHE, (λ > 400 nm)	Photoelectrochemical Hydrogen Evolution	[4]

Pyridine- and tert-Butylthiol-exchange of CdSe Nanocrystals	ligand exchange method	0.2 M Na_2S electrolyte	-75 μA cm^{-2} at 0 mV	photoelectronic applications.	[5]

Table S2 EIS fitting results of the CdS NR's/CdSe-TDH photoanodes synthesized at different hydrothermal times.

Sample/EIS Parameters	R1 (Ω)	R2 (Ω)	CPE1 (μF)	R3 (Ω)	CPE2 (μF)
CdS NR's /CdSe-TDH-2h	2.3	10.06	0.206	623	291.46
CdS NR's /CdSe-TDH-4h	1.37	8.74	0.268	603	673.32
CdS NR's/CdSe-TDH-8h	2.0	12.4	0.258	719	568.36

Table S3 PL lifetime parameters of the CdSe-TDH, $CdSSe(en)_{0.5}$ composite and CdS NR's/CdSe-TDH-4h photoanodes.

Sample	A_1 (%)	τ_1 (ns)	A_2 (%)	τ_2 (ns)	A_3 (%)	τ_3 (ns)	$<\tau>$ [a] (ns)
CdSe-TDH	58	0.08	42	0.26	-	-	0.21
$CdSSe(en)_{0.5}$ composite	46	0.11	53	0.31	1	2.0	0.39
CdS NR's/CdSe-TDH-4h	88	0.61	11	9.0	1	137	73

The time-resolved PL intensity is defined as $I(t) = \sum A_i e^{-t/\tau_i}$, where *I(t)* is the PL intensity as a function of time, *A* is the amplitude, τ is the PL lifetime, and *i* is 2 or 3. [a] The intensity-weighted average lifetime is calculated using $< \tau >= \sum_i A_i \tau_i^2 / \sum_i A_i \tau_i$.[6]

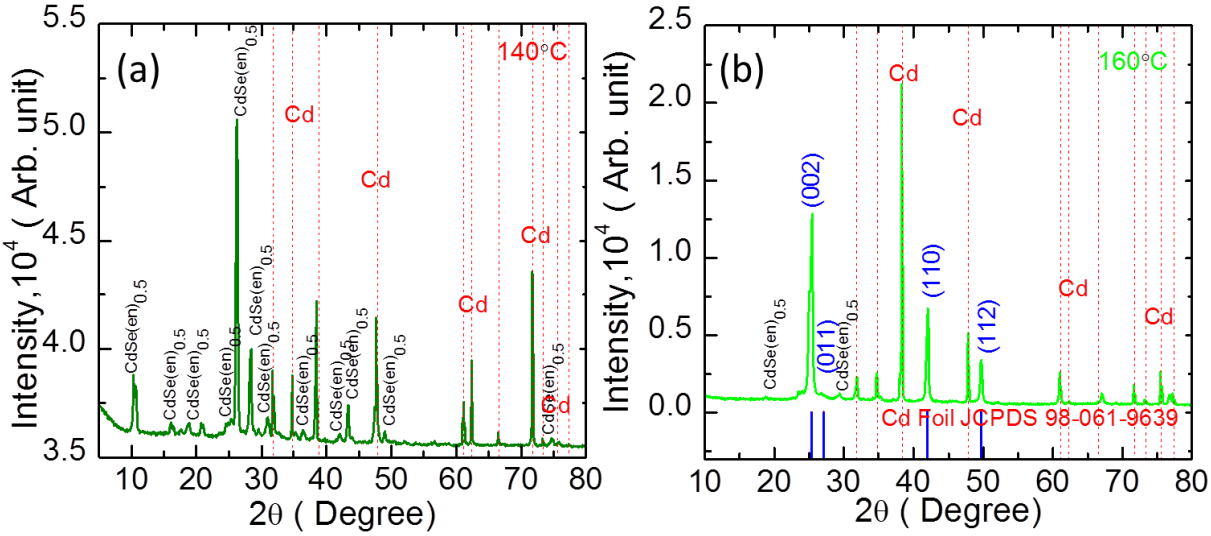

Figure S1 XRD of (a) $CdSe(en)_{0.5}$ nanobelts structures deposited at 140 ^{o}C, 12h, and (b) optimized CdSe-TDH photoelectrodes deposited at 160 ^{o}C, 12h (red dotted lines and Cd indexed for Cadmium foil substrate)

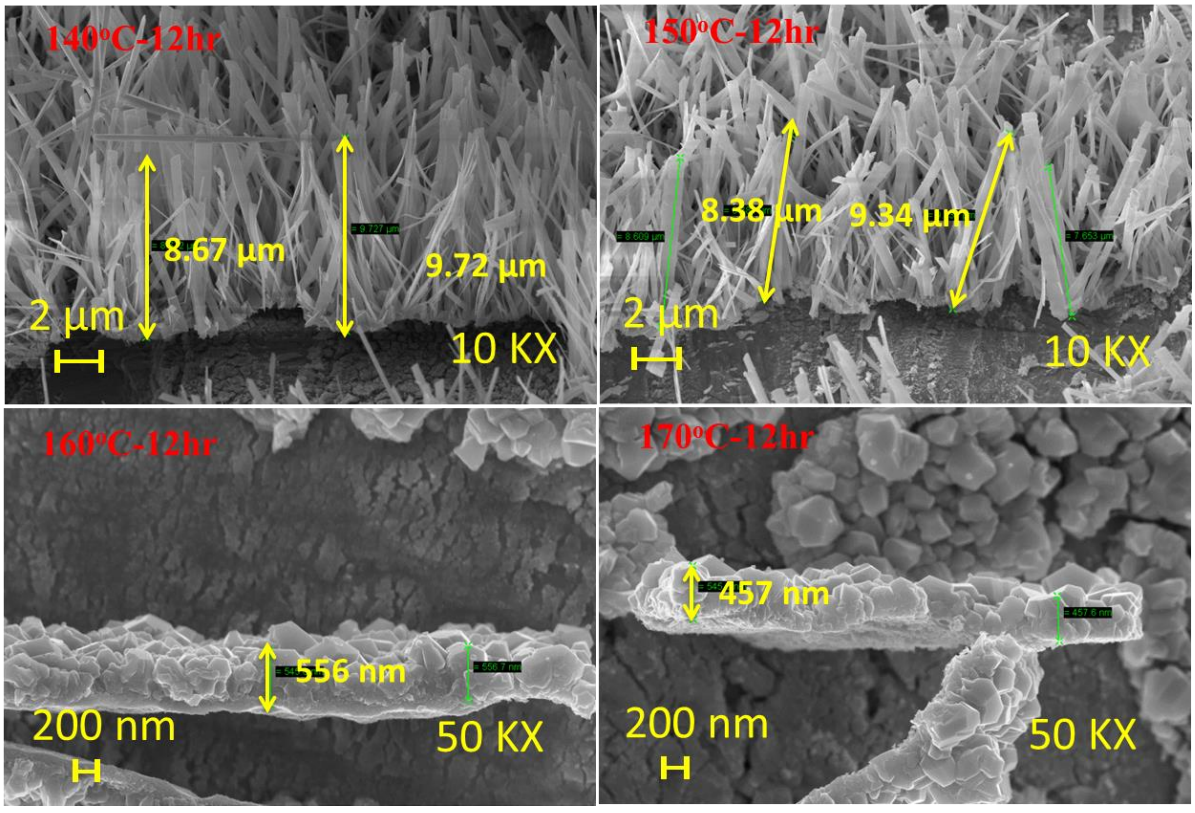

Figure S2 Cross section FESEM images of $CdSe(en)_{0.5}$ nanobelts and CdSe-TDH photoelectrodes films deposited at different hydrothermal temperature.

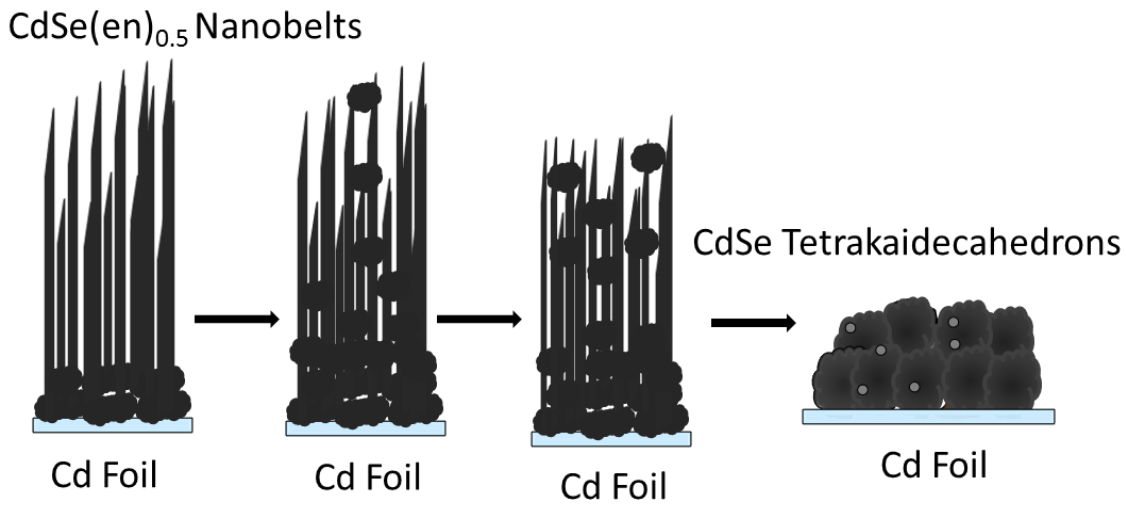

Figure S3 Schematic illustrations for the *in situ* growth mechanism of CdSe-TDH from $CdSe(en)_{0.5}$ nanobelt units.

The possible growth process and transformation of the 1D $CdSe(en)_{0.5}$ nanobelts to CdSe-TDH is proposed in Figure S3. The polished rough surface of Cd foil is assumed to provide the initial nucleation sites to inspire the upward crystal growth, owing to the local enhanced adsorption of reactant ions on its surface.[7, 8] Subsequent growth of CdSe-TDH via $CdSe(en)_{0.5}$ naobelts is effectively mediated by ethylenediamine in solvothermal solution. Ethylenediamine is known to possess a strong chelating capability with metal ions, and meanwhile serve as a capping agent to control the anisotropic growth of $CdSe(en)_{0.5}$ crystal via the selective interaction with specific crystallographic planes.[9] When the solvothermal reaction was more than 140 ^{o}C, the Se was reduced by N_2H_4 group of ethylenediamine to get Se^{2-}) ions as below equation (S1 and S2)[10, 11]:

$$Cd^{2+} + 2en_{(0.5)} \leftrightarrow [Cd(en_{(0.5)})_2]^{2+} \qquad (S1)$$

$$2Se + N_2H_4 + 4OH^- \rightarrow 2Se^{2-} + N_2 \uparrow + 4H_2O \quad (S2)$$

$$[Cd(en_{(0.5)})_2]^{2+} + Se^{2-} \rightarrow CdSe(en)_{0.5} \quad (S3)$$

Lu et al[12] also reported that, due to the strongly nucleophilic properties of ethylenediamine, the development of $Se(en)_{0.5}$ takes place during the solvothermal synthesis $CdSe(en)_{0.5}$. This is due to the formation of the selenium anions (Se^{2-}) when selenium could be reacted and partly reduced by ethylenediamine solvent. Due to more electronegativity of Se than Cd, the interaction of selenium with ethylenediamine forms Se–N covalent bonds. At the same time, the ethylenediamine is also chelated with metal salts (Cd ions) that have already combined with selenium. This process is initial step in the development of the $CdSe(en)_{0.5}$ nanobelt, and is similar to that which occurs when sulfur is activated by amines or hydroxide.13 Thus, selenide (Se^{2-}) could be reacts with the Cd metal foil in the presence of $(en)_{0.5}$, to yield $CdSe(en)_{0.5}$ complex nanobelts (equation S3). As the reaction proceeds at high temperature more than (150 ^oC), the leaflike $CdSe(en)_{0.5}$ nanobelt arrays as sacrificing template units, Se^{2-} in $(en)_{0.5}$ solution react with $CdSe(en)_{0.5}$ nanobelts by diffusing into the nanounits through the leaf apex. With successive ion-exchange reactions between CdSe and $(en)_{0.5}$ solution, the arranged $CdSe(en)_{0.5}$ nanobelt units were dissolved gradually and reorganized into tetrakaidecahedrons forms (equation S4), which is first time reported.

$$CdSe(en)_{0.5} \rightarrow CdSe + (en)_{0.5} \quad (S4)$$

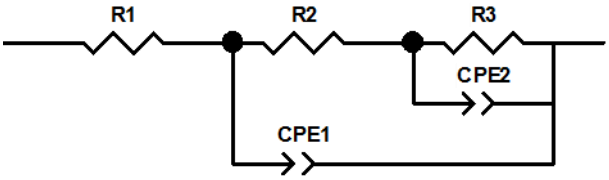

Figure S4 The equivalent circuit used to fit the Nyquist plot using Z-view software.

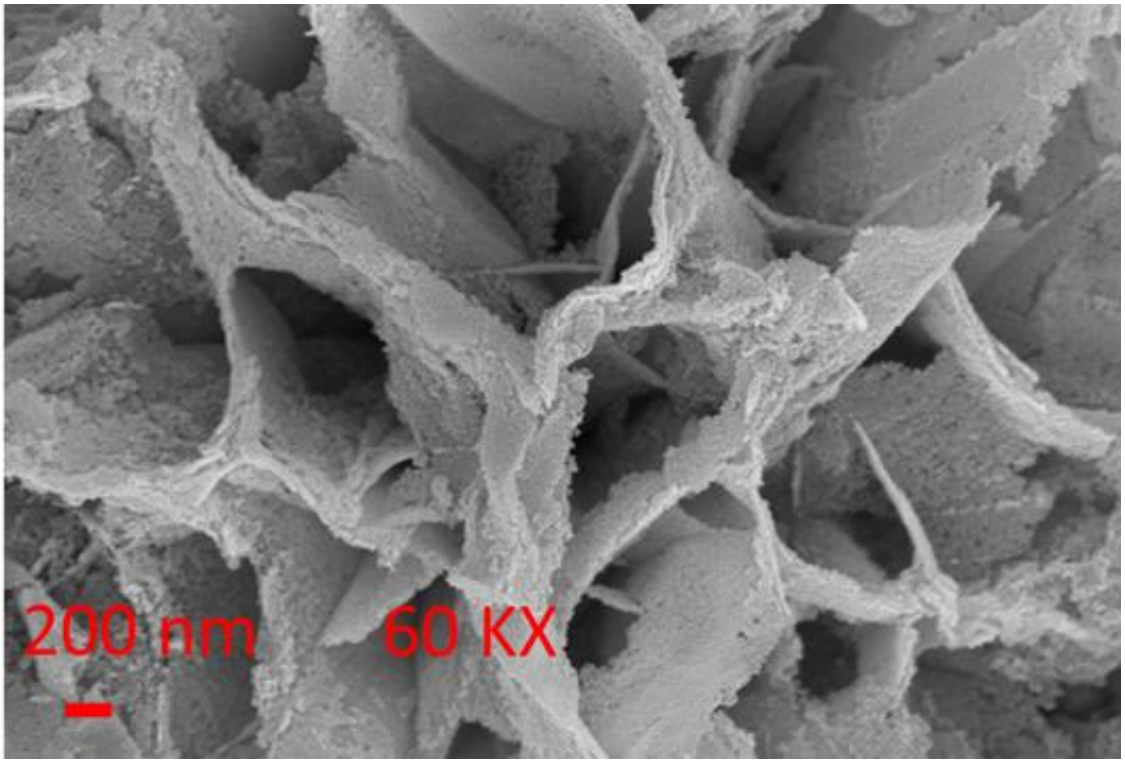

Figure S5. FESEM images of oxygenated CdS NR's/CdSe-TDH heterojunction photoanode deposited at 160 ^{o}C, 4h

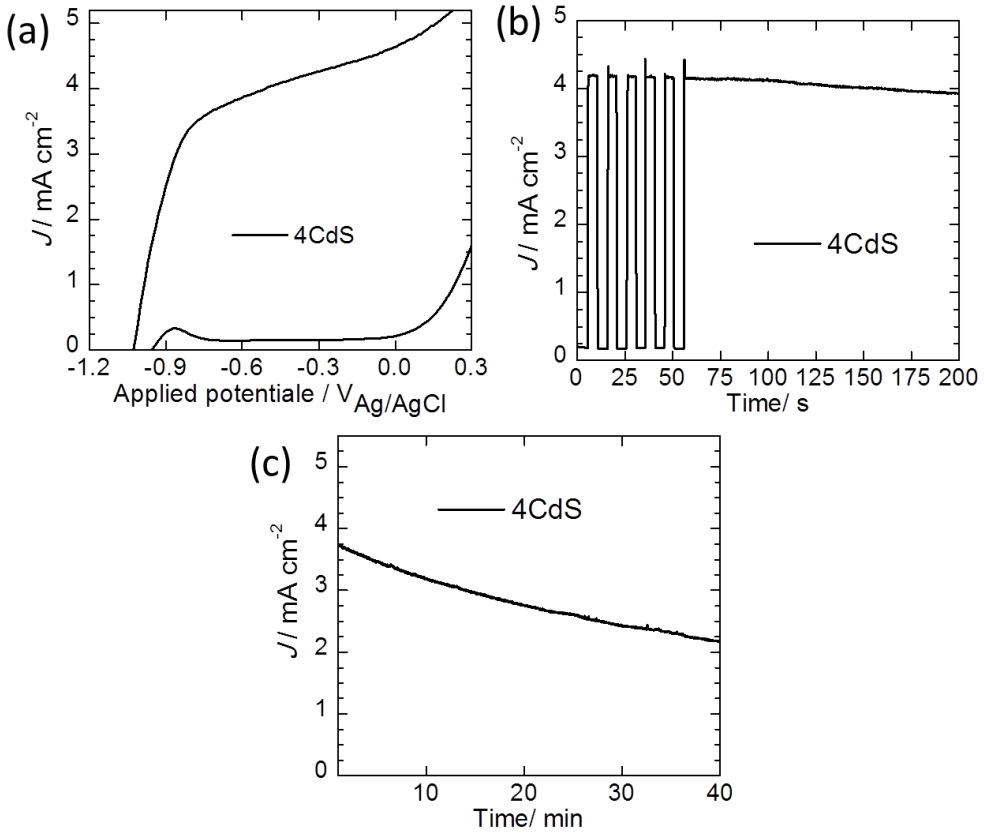

Figure S6 (a) Photocurrent versus applied potential plot (b) amperometric (*J*–*t*) curves of the bare CdS photoanode (4CdS/Cd foil prepared at 160 ^{o}C, 4h, annealed at 300 ^{o}C, 20 min) measured at a 0 V versus Ag/AgCl at 100 mW cm^{-2} with light on–off cycles and (c) stability of corresponding CdS photoanode under continuous illumination.

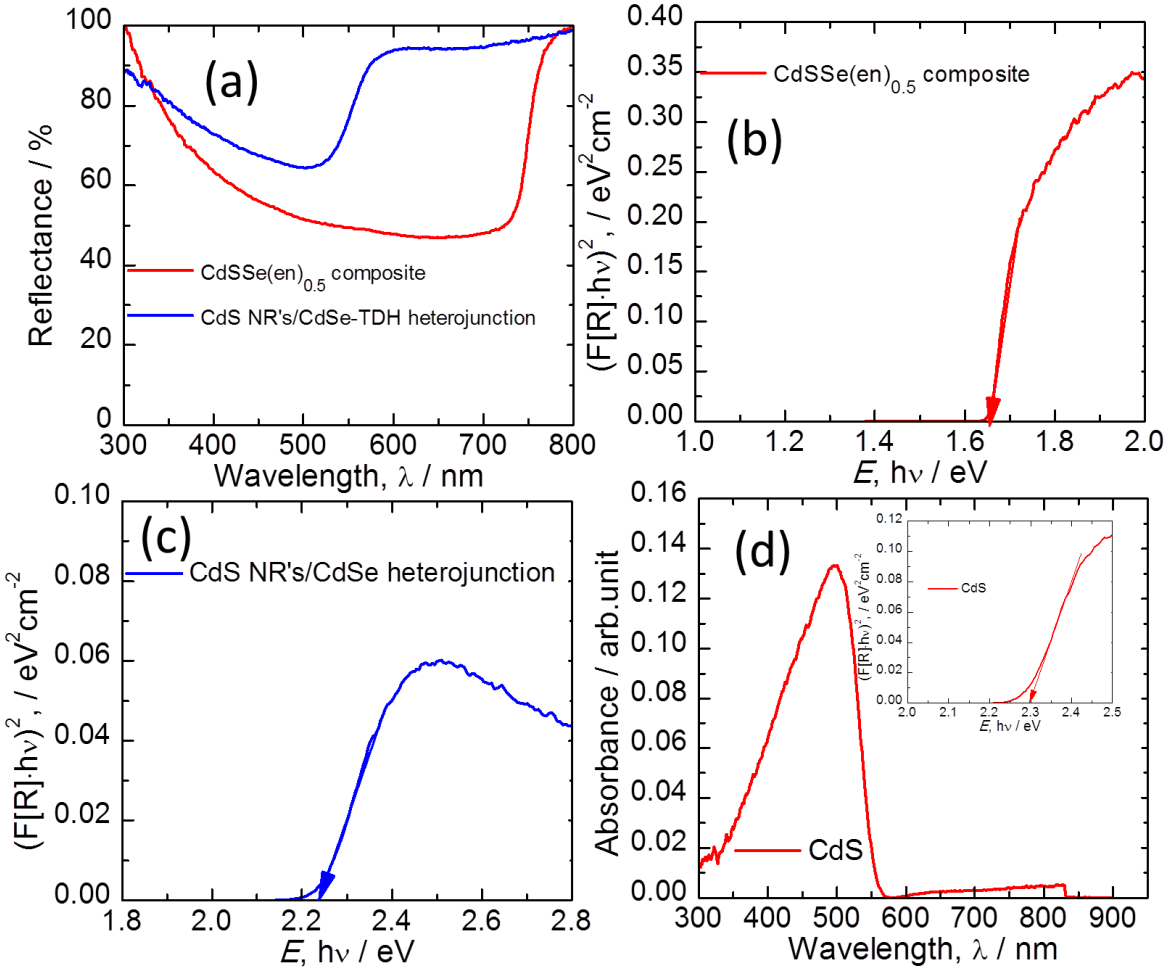

Figure S7. (a) UV-vis reflectance spectrum and (b,c) Tauc plots of $CdSSe(en)_{0.5}$ composite and hydrothermally synthesized CdS NR's/CdSe-TDH heterojunction at 160 ^{o}C, 4 h on Cd foil, (d) UV-vis absorption spectrum of 4CdS/Cd foil annealed at 300 ^{o}C, for 20 min. Inset shows the corresponding Tauc Plot.

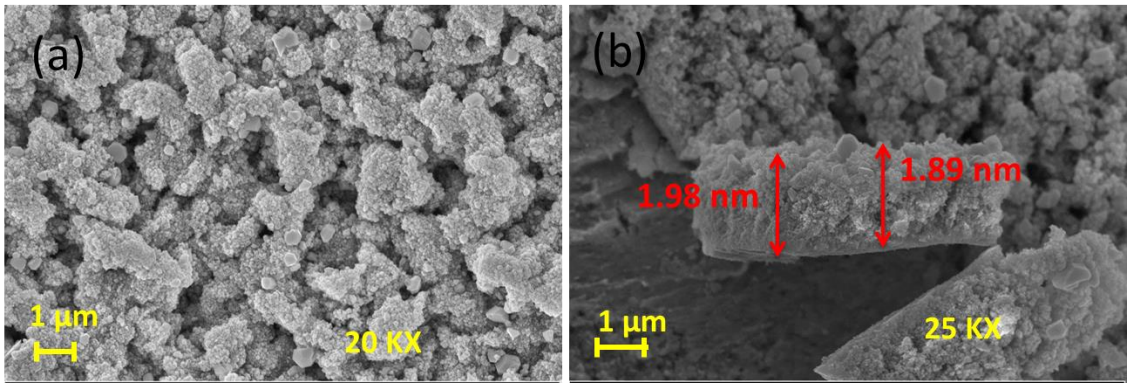

Figure S8. FESEM of $CdSSe(en)_{0.5}$ composite photoanode prepared at 160 ^{o}C, 12h and annealed at 300 ^{o}C, for 20

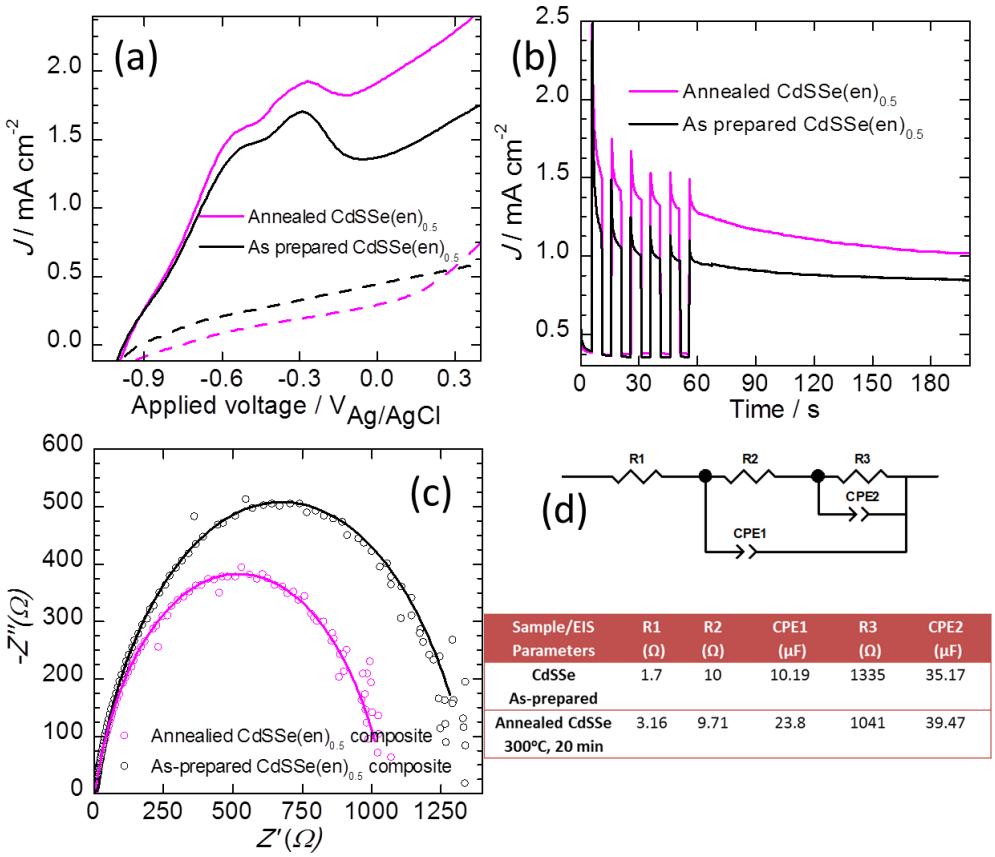

Sample/EIS Parameters	R1 (Ω)	R2 (Ω)	CPE1 (µF)	R3 (Ω)	CPE2 (µF)
CdSSe As-prepared	1.7	10	10.19	1335	35.17
Annealed CdSSe 300°C, 20 min	3.16	9.71	23.8	1041	39.47

Figure S9 (a) LSV, (b) Amperometric (J-t) curves under chopped illumination condition, (c) Nyquist plots of the as-prepared and annealed $CdSSe(en)_{0.5}$ composite under illumination, and (d) corresponding EIS fitting equivalent circuit, where R1 denotes the bulk resistance, originating from the electrolyte and the electrode, R2 of the CPE2 with a high frequency response corresponds to the charge transport in the depletion layer. The impedance response at low to intermediate frequencies (R3, CPE3) is accordingly designated to events occurring in the Helmholtz layer.

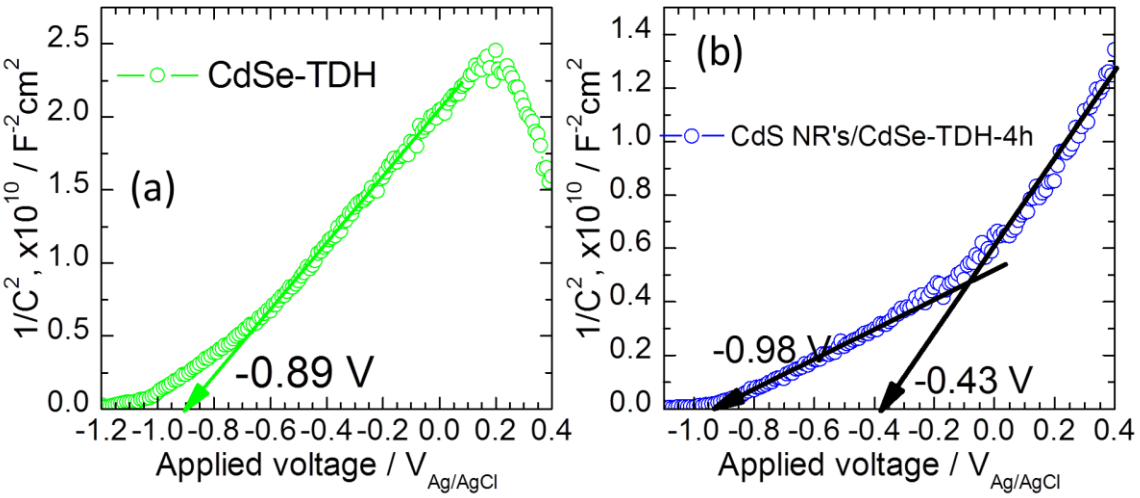

Figure S10 (a,b) Mott–Schottky plots of the CdSe-TDH and CdS NR's/CdSe-TDH heterojunction photoelectrodes annealed at 300 ^{o}C, for 20 min in 0.1 Na_2S+0.01 M Na_2SO_3 solution (pH = 12.8) at 1000 Hz under the dark conditions.

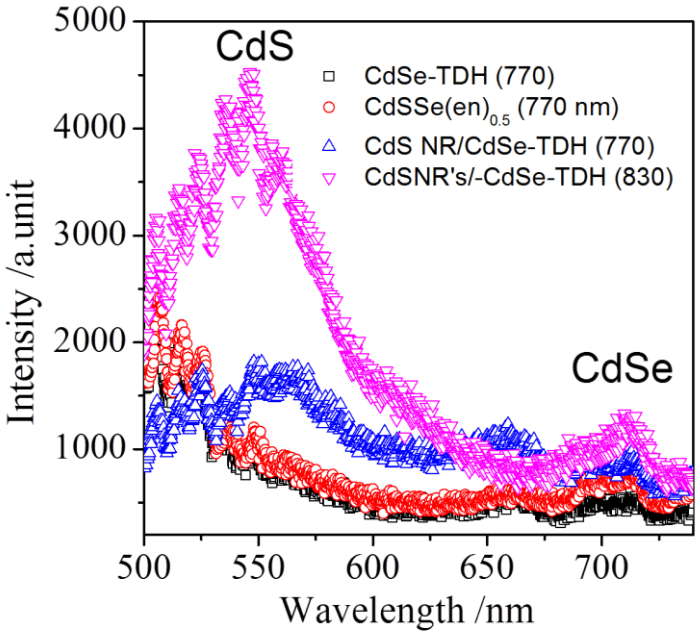

Figure S11. The PL excitation spectrum of the CdSe-TDH, $CdSSe(en)_{0.5}$ composite and CdS NR's/CdSe-TDH-4h heterojunction structure. The value in the parenthesis is detection wavelength. The CdS NR's/CdSe-TDH-4h heterojunction structure showed obviously enhanced contribution from both the CdS and CdSe-TDH phases to the emerged near infrared emission (830 nm) compared to the bare CdSe-TDH and $CdSSe(en)_{0.5}$ composite materials.

References

[1] Abbasi, S.; Molaei, M.; Karimipour, M. CdSe and CdSe/CdS core–shell QDs: New approach for synthesis, investigating optical properties and application in pollutant degradation, *Luminescenc*e, 2017, 32, 1137-1144.

[2] Korala, L.; Wang, Z.; Liu, Y.; Maldonado, S.; Brock, S. L.; Uniform Thin Films of CdSe and CdSe(ZnS) Core(Shell) Quantum Dots by Sol–Gel Assembly: Enabling Photoelectrochemical Characterization and Electronic Applications, *ACS Nano.*,2013, 72, 1215-1223.

[3] Brown, P.; Kamat, P. V. Quantum Dot Solar Cells. Electrophoretic Deposition of CdSe−C60 Composite Films and Capture of Photogenerated Electrons with nC60 Cluster Shell, *J. Am. Chem. Soc*. 2008,130, 8890-8891.

[4] Li, X. B.; Liu, B.; Wen, M.; Gao, Y. J.; Wu, H. L.; Huang, M. Y.; Li, Z. J.; Chen, B.; Tung, C. H.; Wu, L. Z. Hole-Accepting-Ligand-Modified CdSe QD's for Dramatic Enhancement of Photocatalytic and Photoelectrochemical Hydrogen Evolution by Solar Energy, *Adv.Sci*., 2016, 3, 15002821-15002826.

[5] Webber, D. H.; Brutchey, R. L. Ligand Exchange on Colloidal CdSe Nanocrystals Using Thermally Labile tert-Butylthiol for Improved Photocurrent in Nanocrystal Films, *J. Am. Chem. Soc*., 2012,134,1085-1092

[6] Bai, Z.; Yan, X. ; Li, Y.; Kang, Z.; Cao, S.; Zhang, Y. 3D-Branched ZnO/CdS Nanowire Arrays for Solar Water Splitting and the Service Safety Research, *Adv. Energy Mater*., 2016, 6, 1501459.

[7] Yue, J.; Jiang, X.; Yu, A. Molecular Dynamics Study on Metal-Deposited Iron Oxide Nanostructures and Their Gas Adsorption Behavior, *J. Phys. Chem. C*, 2012, 116, 8145–8153.

[8] Kaneti, Y. V.; Zakaria, Q. M. D.; Zhang, Z. ; Chen, C.; Liu, M. Solvothermal synthesis of ZnO-decorated α-Fe_2O_3 nanorods with highly enhanced gas-sensing performance toward n-butanol, *J. Mater. Chem. A*, 2014, 2, 13283-13289.

[9] Deng, H.; Liu, C.; Yang, S.; Xiao, S.; Zhou, Z.; Wang, Q. Additive-Mediated Splitting of Lanthanide Orthovanadate Nanocrystals in Water: Morphological Evolution from Rods to Sheaves and to Spherulites, *Cryst. Growth Des.* 2008, 8, 4432-4439.

[10] Wang, J. W., Deng, Z. X.; Li, Y. D. Synthesis and characterization of Sb_2Se_3 nanorods, *Mater. Res. Bull.* 37, 2002, 495-502.

[11] Liu, Y.; Qiu, H. Y. ; Xu, Y. ; Wu, D.; Li, M. J.; Jiang, J. X. ; Lai, G. Q. Selective synthesis of wurtzite CdSe nanorods and zinc blend CdSe nanocrystals through a convenient solvothermal route, *J. Nanoparticle Res*., 9, 2007,745–752.

[12] Lu, J.; Xie, Y.; Xu, F.; Zhu, L. Study of the dissolution behavior of selenium and tellurium in different solvents—a novel route to Se, Te tubular bulk single crystals, *J. Mater. Chem*., 2002, 12, 2755–2761.

[13] Jiang, T.; Ozin, G. A.; Bedard, R. L. Nanoporous tin(IV) sulfides: Mode of formation, *Adv. Mater.*, 1994, 6, 860-865.